# Hybrid MoM/SBR Method to Compute Scattering from a Slot Array Antenna in a Complex Geometry

Andrew D. Greenwood* and Jian-Ming Jin
Center for Computational Electromagnetics
Department of Electrical and Computer Engineering
University of Illinois
Urbana, Illinois 61801

*Also affiliated with Air Force Research Laboratory at Rome/IFSB, Rome, NY 13441

**Abstract**

A method of moments (MoM) code has been developed to compute the scattering from a planar or cylindrically conformal slot array antenna. By hybridizing the MoM with the shooting and bouncing ray (SBR) method, the scattering from a large, complex target with a slot array antenna can be computed. The scattering problem can be decomposed using the field equivalence principle such that the MoM is employed to model the slot array while the SBR method is used to compute the scattering from the large, complex target. Sample results show the utility of the method and the need to include slot array scattering when computing the RCS of a complex target.

## 1 Introduction

The presence of a slotted waveguide array antenna on a radar target may have a significant contribution to the overall radar cross-section (RCS) of the target. Therefore, the computation of the RCS should include the scattering from the slot array. Recently, a method of moments (MoM) procedure has been introduced to compute the scattering from a cylindrically conformal slotted-waveguide array antenna [1, 2]. However, this procedure does not take into account the geometry in which the slot array is located. If the slot array is located in a complex, three-dimensional (3-D) geometry, the MoM cannot efficiently account for the effect of the geometry. A more efficient method to compute the scattering from a large, 3-D body is the high frequency shooting-and-bouncing-ray (SBR) method. However, this method cannot accurately account for the slots, each of which is typically smaller than an electromagnetic wavelength in size. In this paper, the MoM computation of the scattering from a slot array is hybridized with the SBR method to compute the electromagnetic scattering from a large, 3-D target which includes a slot array antenna.

The basis of the hybrid method is the field equivalence principle, which allows the scattering geometry to be decomposed into separate regions. The MoM is applied to the slotted waveguides, while the SBR method is applied to the region outside the waveguides, which includes the complex, 3-D target. By using the hybrid method, the scattering from a large, 3-D target, which includes a slotted-waveguide array antenna, can be efficiently and accurately computed.

The remainder of this paper is divided into four sections. Section 2 describes the formulation of the problem, including the use of the MoM, the use of the SBR method, and techniques to decouple the computations of the two methods. Section 3 describes briefly how the method has been tested, and Section 4 gives some numerical results which show the capability of the method. The results in Section 4 also demonstrate the need to include the slot array in scattering computations. Finally, Section 5 gives a brief conclusion.

## 2 Formulation

Consider the example target shown in Figure 1a. The target is complex and 3-D, and it includes a slotted waveguide array antenna on its surface. The slotted waveguide array antenna may be planar, or it may conform to the surface of a cylinder. The first step to compute the scattering from this target is to analyze the slotted waveguides using the MoM. Then, the scattering from the target with the slot apertures covered by perfect electric conductor (PEC) is computed using the SBR method. During the SBR calculation, the incident field on the slot array antenna is computed and stored. This incident field is combined with the MoM analysis to find an equivalent magnetic current on the outer aperture of each slot. Finally, the radiation of these equivalent magnetic currents in the presence of the complex, 3-D target is computed using the reciprocity theorem. This result is added to the previously computed SBR scattering result.

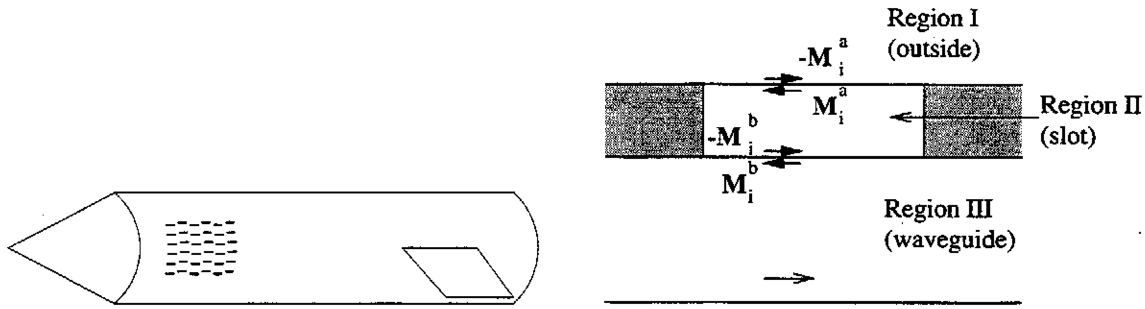


(a) Large target

(b) Local slot geometry

Figure 1: Example of a complex, 3-D target with a slot array antenna and the local slot geometry.

## 2.1 Use of MoM

The first step in the formulation of the problem is to analyze the slotted waveguides using the MoM. There are two main steps in the application of the MoM. First, the problem must be described in terms of an integral equation. Then, the integral equation is discretized to find a numerical solution. The steps are outlined here, and more detail is given in [1, 2].

To derive the integral equation, the apertures of each slot are first covered with PEC, and equivalent magnetic currents over each aperture are introduced. Figure 1b depicts the situation for the $i^{th}$ slot. The region outside of the antenna is denoted Region I, the region inside the slot is Region II, and the region outside of the slot but inside the waveguide is Region III. An equivalent magnetic current $\mathbf{M}_i^a$ is introduced on the inside of the outer slot aperture (between Regions I and II), and the equivalent current $\mathbf{M}_i^b$ is introduced on the waveguide side of the inner aperture (between Regions II and III). Because the electric field must be continuous across each aperture, $-\mathbf{M}_i^a$ must be introduced on the outside of the outer aperture, and $-\mathbf{M}_i^b$ must be introduced on the slot side of the inner aperture. Note that when the analysis is completed, $-\mathbf{M}_i^a$ are the currents that radiate in the presence of the complex, 3-D body as discussed above.

To derive the integral equation, the continuity of the tangential magnetic field across each aperture is enforced. Denoting the tangential magnetic field in Region III on the $i^{th}$ slot aperture due to the magnetic current on the $j^{th}$ aperture as $\mathbf{H}_{\tau i}^{\mathrm{III}}(\mathbf{M}_j^b)$, the following must hold on each inner aperture:

$$\sum_j \mathbf{H}_{\tau i}^{\mathrm{III}}(\mathbf{M}_j^b) + \mathbf{H}_{\tau i}^{\mathrm{II}}(\mathbf{M}_i^b) - \mathbf{H}_{\tau i}^{\mathrm{II}}(\mathbf{M}_i^a) = 0. \qquad (1)$$

Further, denoting the tangential incident field on the $i^{th}$ slot aperture as $\mathbf{H}_{\tau i}^{\mathrm{SBR}}$,

$$\sum_j \mathbf{H}_{\tau i}^{\mathrm{I}}(\mathbf{M}_j^a) + \mathbf{H}_{\tau i}^{\mathrm{II}}(\mathbf{M}_i^a) - \mathbf{H}_{\tau i}^{\mathrm{II}}(\mathbf{M}_i^b) = \mathbf{H}_{\tau i}^{\mathrm{SBR}} \qquad (2)$$

must hold on each outer slot aperture. Note that the incident fields are calculated using the SBR method, and the magnetic field due to a magnetic current is found from

$$\mathbf{H}^\alpha(\mathbf{M}) = \iint_S \overline{\overline{G}}^\alpha(\mathbf{r},\mathbf{r}') \cdot \mathbf{M}(\mathbf{r}')dS' \qquad (3)$$

where $\alpha$ is I, II, or III, depending on the region of interest, $\overline{\overline{G}}^\alpha(\mathbf{r},\mathbf{r}')$ is the magnetic-source-magnetic-field dyadic Green's function in the appropriate region, and $\mathbf{r}$ corresponds to the point at which the magnetic field is to be evaluated. Combining Equations 1, 2, and 3 gives an integral equation for the magnetic currents.

The second main step in application of the MoM is to discretize the integral equation to find a numerical solution for the currents. To accomplish this step, the currents are expanded in terms of sinusoidal basis functions. Defining $\hat{\xi}$ to be the direction parallel to the lengths of the slots and using a local coordinate system in which $\xi_j = 0$ at one end of the $j^{th}$ slot, the current on the $j^{th}$ slot aperture is expanded as

$$\mathbf{M}_j^\beta = \hat{\xi} \sum_{q=1}^{N} V_{qj}^\beta \sin\left(\frac{q\pi}{L_j}\xi_j\right) \qquad (4)$$

where $N$ is the number of terms in the expansion, and $\beta$ represents $a$ for the current on the outer aperture or $b$ for the current on the inner aperture. Equation 4 is valid for points on the $j^{th}$ slot aperture; for points outside of the aperture, the expansion is defined to be zero. Assuming the width of a slot is much less than its length, the $\hat{\xi}$ component of the current is the only component of interest.

Substituting the expansion given in Equation 4 into the integral equation allows the integral equation to be converted to a matrix equation which can be solved numerically. For more details about solving the integral equation, the reader is referred to [1,2]. However, one important step that should be mentioned here is the derivation of the dyadic Green's functions for the various regions. The Green's functions given in [1,2] for Regions II and III are applicable to the present problem. For Region I, the dyadic Green's function can be written as

$$\overline{\overline{G}}^{\mathrm{I}}(\mathbf{r},\mathbf{r}') = \overline{\overline{G}}^{\mathrm{cyl}}(\mathbf{r},\mathbf{r}') + \overline{\overline{G}}^{\mathrm{diff}}(\mathbf{r},\mathbf{r}'). \qquad (5)$$

The Green's function given in [1,2] for the exterior region corresponds to $\overline{\overline{G}}^{\mathrm{cyl}}(\mathbf{r},\mathbf{r}')$, and $\overline{\overline{G}}^{\mathrm{diff}}(\mathbf{r},\mathbf{r}')$ is a perturbation term due to diffraction and reflection by the complex target in which the slot array is embedded. Neglecting $\overline{\overline{G}}^{\mathrm{diff}}(\mathbf{r},\mathbf{r}')$ neglects fields which are scattered by the slots, diffracted or reflected by the large body back to the slots, and scattered by the slots again [3]. These fields are usually an insignificant part of the scattering, and this term is neglected in the computations. Thus, the Green's function given in [1,2] for Region I is used for the present problem.

## 2.2 Use of SBR

As previously mentioned, the MoM is used to analyze the slot array antenna while the SBR method is used for the remainder of the problem. Thus, there are three main tasks to be accomplished by the SBR method: to compute the scattering from the complex, 3-D target, to compute the incident magnetic fields on the slot apertures, and to compute the radiation of the equivalent currents on the slot apertures in the presence of the complex, 3-D target. In all of these cases, the slot apertures are covered with PEC.

The details of the SBR method are discussed in [3–6]. For the present problem, the SBR procedure is used to compute the scattering from the complex, 3-D target with the slot apertures closed by PEC. The SBR procedure is implemented using the XPATCH software package [4,5].

The incident magnetic field on the slot apertures is computed using SBR at the same time the scattering from the complex, 3-D target is computed. While tracing the rays to find the scattering, some rays will hit on or near a slot aperture. The field contributions from each of these rays are combined with appropriate phase shifts to find the incident magnetic field on each slot aperture. The incident magnetic fields on the slot apertures are used by the MoM to compute the equivalent magnetic currents on the apertures.

The remaining step in the problem is to compute the radiation of the magnetic currents in the presence of the large body. The SBR method together with the reciprocity theorem is employed for this task [3,6]. Consider an infinitesimal dipole placed at the scattering observation point. If the target containing the slot array is in the far field of the dipole, the dipole launches a plane wave toward this target. Recall that for the SBR method, the grid of rays launched toward the target corresponds to a plane wave. Note also that the reciprocity theorem states

$$\iiint_V \mathbf{E}^{\mathrm{Slot}} \cdot \mathbf{J}\,dV = \iint_S \mathbf{H}_\tau^{\mathrm{SBR}} \cdot \mathbf{M}^a\,dS \qquad (6)$$

where $\mathbf{H}_\tau^{\mathrm{SBR}}$ is the incident field on the slot apertures due to the dipole at the scattering observation point, $\mathbf{M}^a$ is the current on the outer slot apertures, which is found using the MoM, $\mathbf{E}^{\mathrm{Slot}}$ is the radiation due to $-\mathbf{M}^a$, and $\mathbf{J}$ is the dipole current. Thus, if the dipole current ($\mathbf{J}$) is appropriately chosen and mono-static scattering is being computed, all components to find $\mathbf{E}^{\mathrm{Slot}}$ using reciprocity are computed already. If bi-static scattering results are desired, $\mathbf{H}_\tau^{\mathrm{SBR}}$ resulting from a dipole at the scattering observation point must be computed first, then $\mathbf{E}^{\mathrm{Slot}}$ can be computed.

## 2.3 Decoupling the MoM from the SBR Method

As they are presented in Section 2.1, the MoM computations are coupled to the SBR method computations. This is due to the fact that the incident magnetic field on the slot apertures, which is computed using the SBR method, is required for the MoM computations. To avoid having to repeat the MoM computations in order to analyze the scattering from many different incidence angles, it is desirable to decouple the computations of the two methods. There are two ways of doing this. The first method preserves the coupling interactions between different slots; the second involves an approximation which neglects the coupling between different slots to achieve lower computational complexity.

To decouple the MoM computations from the SBR computations while preserving the coupling between the various slots, the incident magnetic field on the slot apertures can be expanded in terms of basis functions. Assuming that the width of a slot is much less than its length, the component of the incident magnetic field along the length of a slot is the only component of interest. A convenient basis set is the set of pulse basis functions, where each function is defined to be one on a portion of a single slot aperture and zero elsewhere. The magnetic currents on each slot aperture are then computed with the incident field on the slot array set equal

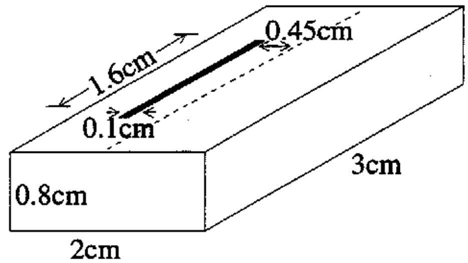


(a) Geometry

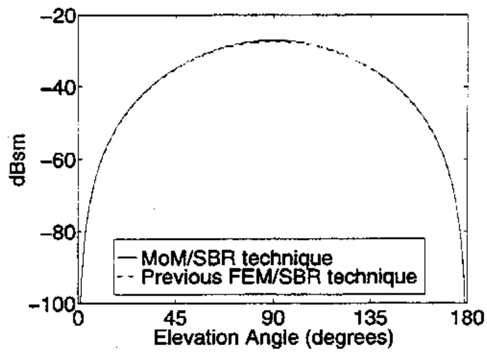


(b) Magnitude

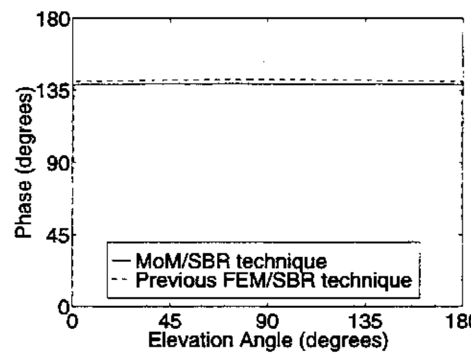


(c) Phase

Figure 2: Comparison between the proposed MoM/SBR technique and a previously published FEM/SBR technique. The scattering results are computed at a frequency of 8 GHz, and the scattering contribution of the slot only is shown.

to each of the basis functions in turn. A matrix-vector multiply is then carried out during the SBR computations. This matrix-vector multiply converts the incident magnetic fields on the slot apertures to the equivalent currents on the apertures.

The second method of decoupling the MoM computations from the SBR computations neglects the coupling between the individual slots. One slot on the array is chosen, and it is assumed that this slot is the only one present. The MoM computation is carried out with a magnetic field of unit amplitude on the chosen slot, and the result is a magnetic current on the aperture. It is then assumed that all of the slots in the array are equivalent; the magnetic current on each one is set equal to the incident magnetic field times the single magnetic current computed by the MoM. This approximation significantly reduces the computational complexity and the sizes of data files. However, it does not produce accurate results when the frequency is near the working frequency of the slot array. This is demonstrated in Section 4.

# 3 Testing

Before using any new numerical technique, the technique should be tested against measurements or alternate techniques to ensure its validity. Ideally, measured data is used for comparison, but unfortunately measured data for this problem is unavailable. However, the validity of the MoM computation involving the coupling between the different slots in the array is validated by comparison with previous MoM and finite-element method (FEM) techniques [2,7]. The SBR method is also validated through extensive, previous testing [4,5]. The hybrid technique is validated by comparison with a previous hybrid method to compute the scattering from complex targets with cracks and cavities on their surfaces [3]. The comparison is accomplished by considering a waveguide with each end terminated by a (short-circuit) PEC plate and with a single slot on the waveguide surface. The geometry is shown in Figure 2a. The waveguide with a single slot can be modeled both as a slotted cavity for the FEM technique and as a slotted waveguide for the MoM technique. Figures 2b and 2c show a comparison of

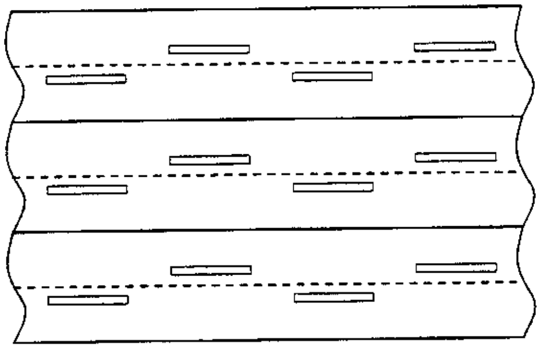

Figure 3: Configuration of the slots on the surface of waveguides.

the magnitude and the phase of the backscattered field from the slot in the presence of the waveguide. There is good agreement both in magnitude and in phase. Both magnitude and phase agreement are important so that when the scattered field from the external geometry is added, correct results are produced.

# 4 Numerical Examples

To show the capability and utility of the proposed technique, several numerical results are presented. For all of the numerical examples, the slot array contains 16 waveguides with 16 slots on each waveguide, and the array is designed to radiate at 9.1 GHz. In addition, the following parameters apply to all of the examples presented: the upper waveguide wall in which the slots are cut is 0.08 cm thick, the waveguides are separated by walls 0.1 cm thick, each slot is 1.6 cm long and 0.16 cm wide, and the slots are positioned on the waveguide surface as shown in Figure 3, where the offset of each slot from the center of the waveguide is 0.15 cm. Unless otherwise noted, the coupling between individual slots in the array is included in the results.

The first example is a planar slot array sitting on a simple ground plane. The waveguides are 2.230 cm wide by 1.016 cm high, the slot centers are 2.444 cm apart, and the first and last slot centers are 1.222 cm from the ends of the waveguides. Thus, the entire slot array and the ground plate are 37.3 cm wide by 39.1 cm long. In Figure 4, the RCS of the plate with the slots is superimposed on the scattering from the plate alone. The scattering frequency is 9.1 GHz, which is the working frequency of the slot array. Figure 4 shows results in both the $H$-plane and the $E$-plane and for waveguides which are terminated both with matched loads and with short circuits. For matched waveguide loads, each waveguide is terminated with an impedance sheet which is matched to the characteristic impedance of the guide. In the case of short circuit waveguide loads, each waveguide is terminated with a PEC plate. For some incidence angles, the slot array has a dominant effect on the scattering.

The second example is a slot array on a cylinder with a nose cone. The radius of the cylinder is 16.096 cm, and the length without the nose cone is 100 cm. The nose cone is 30 cm long. The waveguide cross-sections are sectoral in shape and are 1.016 cm thick. Along the slotted surface, the waveguides are 2.230 cm wide. The slots are 2.573 cm apart, and the first and last slots are 1.287 cm from the ends of the waveguides. The entire slot array is 37.3 cm along the circumference of the cylinder and 41.2 cm along the axis of the cylinder. In Figure 5, the $H$-plane RCS of the cylinder alone and the RCS of the cylinder with the slot array are compared. The scattering frequency is 9.1 GHz, the working frequency of the slot array, and again, there are scattering directions for which the slot array dominates the return.

The next example is intended to show the effect of the uncoupled slot approximation which was discussed in Section 2.3. Figure 6 shows the RCS of the same geometry considered in the second example, but as a function of frequency. The incident direction is 40° in the $H$-plane. The RCS computed considering the coupling between individual slots is plotted with the RCS computed by neglecting the slot coupling. The approximation neglecting slot coupling is reasonably accurate away from the working frequency of the slot array antenna, but there is significant error near the working frequency. Thus, this approximation must be applied with care.

The final example shows the usefulness of the method. The planar slot array antenna from the first example is mounted in the nose cone of an aircraft. Figure 7a shows the aircraft, and Figures 7b and 7c show the HH-polarized range profile of the airplane both with and without the slot array. The range profile is the time domain response to an incident sinc pulse. The sinc pulse in this example has a center frequency of 10 GHz and a bandwidth of 4 GHz, and the slot array has shorted waveguide loads. The slot scattering has an impact on

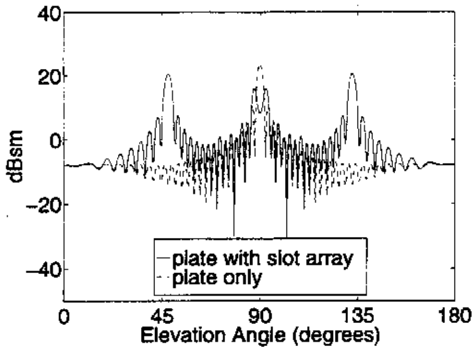


(a) $H$-plane, matched waveguide loads

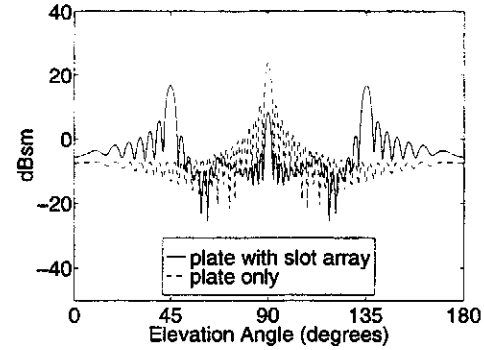


(b) $E$-plane, matched waveguide loads

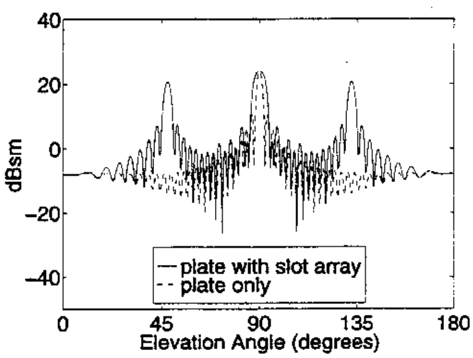


(c) $H$-plane, short-circuit waveguide loads

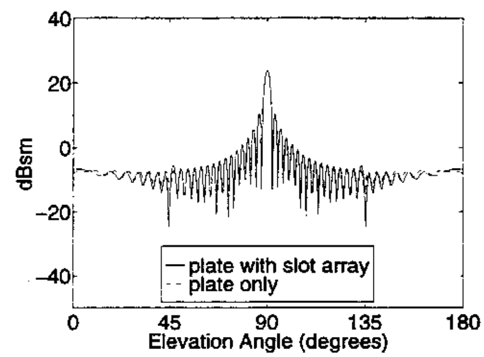


(d) $E$-plane, short-circuit waveguide loads

Figure 4: RCS of a planar slot array on a ground plate at 9.1 GHz, the working frequency of the slot array.

the range profile.

# 5 Conclusion

A hybrid MoM/SBR method is developed to compute the scattering from a complex, 3-D target with a slotted waveguide array antenna. Because the target is large and 3-D, the MoM alone cannot efficiently compute the scattering, and because the slots on the waveguides are small features, the SBR method alone is not accurate. The hybrid method combines the two individual methods in such a manner that the scattering can be efficiently and accurately computed. In the hybrid method, the MoM is used to model the details of the slot array, and the SBR method is used to model the electromagnetic interactions with the large, complex target. The method is validated by comparison to previously published methods. Numerical examples show the need to include a slot array model when computing the scattering from a complex target with a slotted waveguide array. The examples also illustrate the capability of the method.

**Acknowledgments:** This work was supported by the Office of Naval Research under grant N00014-95-1-0848 and by NASA under grant NAG3-1474. Dr. G. X. Fan's contribution to the development of the computer code for slot array scattering is acknowledged.

# References

[1] G. X. Fan and J. M. Jin, "Scattering from a cylindrically conformal slotted-waveguide array antenna," *IEEE Antennas and Propagation Society International Symposium Digest*, pp. 1394–1397, 1996.

[2] G. X. Fan and J. M. Jin, "Scattering from a cylindrically conformal slotted-waveguide array antenna," *IEEE Trans. Antennas Propagat.*, vol. 45, no. 7, pp. 1150–1159, Jul. 1997.

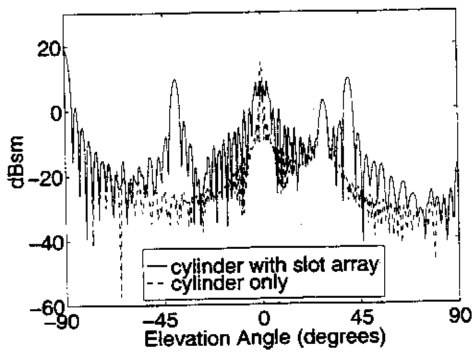


(a) Matched waveguide loads

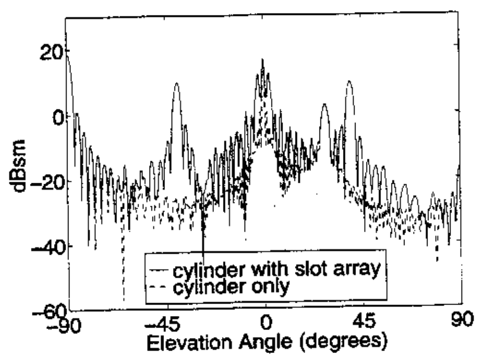


(b) Short-circuit waveguide loads

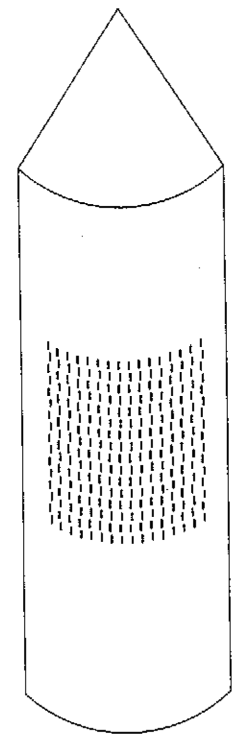

(c) Geometry

Figure 5: RCS of a conformal slot array on a cylinder with a nose cone at 9.1 GHz, the working frequency of the slot array.

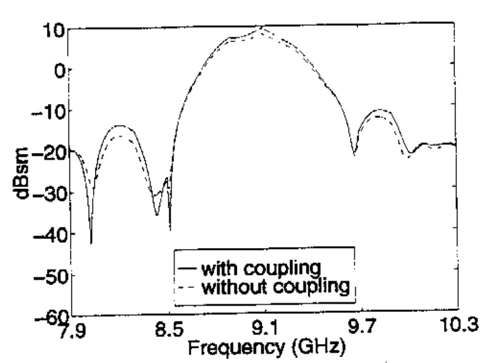


(a) Matched waveguide loads

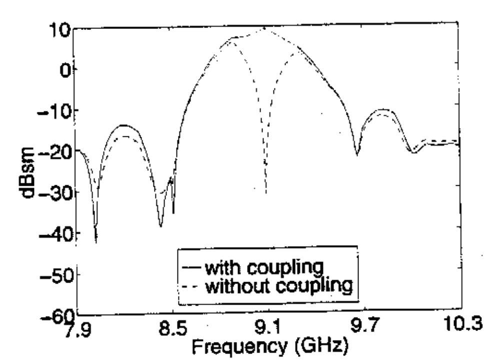


(b) Short-circuit waveguide loads

Figure 6: RCS of a conformal slot array on a cylinder with a nose cone. The scattering is computed with and without including the coupling between individual slots. Near the working frequency of the slot array (9.1 GHz), the slot coupling has a significant effect.

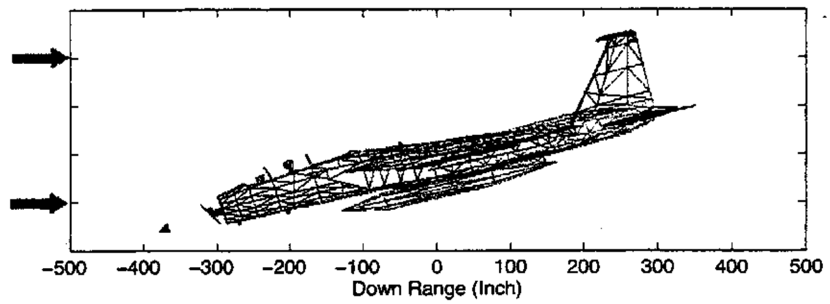


(a) Aircraft geometry.

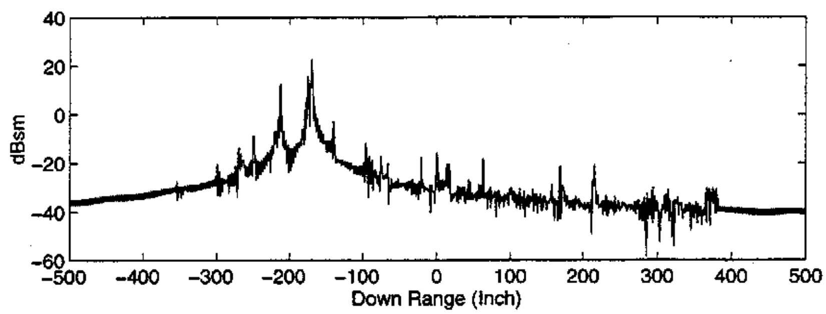


(b) Range profile without slot array.

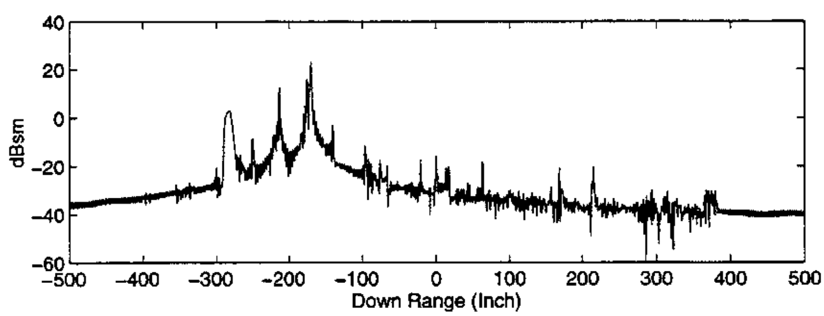


(c) Range profile with slot array.

Figure 7: Range profile of an aircraft, 15° elevation, 0° azimuth, HH-polarization, 10 GHz center frequency, 4 GHz bandwidth. The slot array has shorted waveguide loads.

[3] J. M. Jin, S. S. Ni, and S. W. Lee, "Hybridization of SBR and FEM for scattering by large bodies with cracks and cavities," *IEEE Trans. Antennas Propagat.*, vol. 43, no. 10, pp. 1130–1139, Oct. 1995.

[4] S. W. Lee, D. J. Andersh, D. D. Reeves, S. K. Jeng, H. Ling, Y. Chu, D. P. Sullivan, and C. L. Yu, "User manual for XPATCH," DEMACO, Inc., Champaign, IL, 1993.

[5] D. J. Andersh, M. Hazlett, S. W. Lee, D. D. Reeves, D. P. Sullivan, and Y. Chu, "XPATCH: A high-frequency electromagnetic-scattering prediction code and environment for complex three-dimensional objects," *IEEE Antennas Propagat. Mag.*, vol. 36, no. 1, pp. 65–69, Feb. 1994.

[6] A. D. Greenwood, S. S. Ni, J. M. Jin, and S. W. Lee, "Hybrid FEM/SBR method to compute the radiation pattern from a microstrip patch antenna in a complex geometry," *Microwave and Optical Technology Letters*, vol. 13, no. 2, pp. 84–87, Oct. 1996.

[7] J. Chen and J. M. Jin, "Electromagnetic scattering from slot antennas on waveguides with arbitrary terminations," *Microwave and Optical Technology Letters*, vol. 10, no. 5, pp. 286–291, Dec. 1995.